Article

RGD-FasL Induces Apoptosis in Hepatocellular Carcinoma

Zhongchen Liu[1, 3, 4], Juan Wang[1, 2, 4], Ping Yin[3], Jinhua Qiu[1], Ruizhen Liu[1], Wenzhu Li[1, 2], Xin Fan[1], Xiaofeng Cheng[1], Caixia Chen[1, 2], Jiakai Zhang[2] and Guohong Zhuang[1, 5]

Despite impressive results obtained in animal models, the clinical use of Fas ligand (FasL) as an anticancer drug is limited by severe toxicity. Systemic toxicity of death ligands may be prevented by using genes encoding membrane-bound death ligands and by targeted transgene expression through either targeted transduction or targeted transcription. Selective induction of tumor cell death is a promising anticancer strategy. A fusion protein is created by fusing the extracellular domain of Fas ligand (FasL) to the peptide arginine-glycine-aspartic acid (RGD) that selectively targets avβ3-integrins on tumor endothelial cells. The purpose of this study is to evaluate the effects of RGD-FasL on tumor growth and survival in a murine hepatocellular carcinoma (HCC) tumor model. Treatment with RGD-FasL displaying an obvious suppressive effect on the HCC tumor model as compared to that with FasL ($p < 0.05$) and resulted in a more additive effect on tumor growth delay in this model. RGD-FasL treatment significantly enhanced mouse survival and caused no toxic effect, such as weight loss, organ failure, or other treatment-related toxicities. Apoptosis was detected by flow cytometric analysis and TUNEL assays; those results also showed that RGD-FasL is a more potent inducer of cell apoptosis for H22 and H9101 cell lines than FasL ($p < 0.05$). In conclusion, RGD-FasL appears to be a low-toxicity selective inducer of tumor cell death, which merits further investigation in preclinical and clinical studies. Furthermore, this approach offers a versatile technology for complexing target ligands with therapeutic recombinant proteins. To distinguish the anti-tumor effects of FasL *in vivo*, tumor and liver tissues were harvested to examine for evidence of necrotic cells, tumor cells, or apoptotic cells by Hematoxylin and eosin (H&E) staining. *Cellular & Molecular Immunology*. 2009;6(4):285-293.

Key Words: FasL, RGD-FasL, apoptosis, tumor targeting

Introduction

Hepatocellular carcinoma (HCC) is one of the most common cancers and has an extremely poor prognosis because of its aggressive invasion, resistance to existing chemotherapeutic agents, and lack of specific symptoms. Hepatitis B virus (HBV) infects approximately two billion individuals worldwide and causes an estimated 320,000 deaths annually. Approximately 30%-50% of HBV-related deaths are attributable to HCC (1). Traditionally, chemotherapy is the primary option for the treatment of unresectable solid tumors; however, these drugs are not effective in promoting tumor regression and prolonging survival in HCC (2). Moreover, conventional therapeutic modalities, such as transcatheter arterial embolization, radiofrequency ablation, and microwave coagulation therapy are no longer recommended because of their low efficacy and potential complications (3). Therefore, a new effective modality is needed to treat HCC.

Apoptosis, or programmed cell death, is a key mechanism that multicellular organisms utilize to regulate cell growth and to prevent pathological processes, such as autoreactivity, cancer, and immunodeficiency (4). Fas ligand (FasL), a type II membrane protein, belongs to the tumor necrosis factor (TNF) superfamily. FasL is expressed by activated T lymphocytes, natural killer (NK) cells, and a small number of

[1]Anti-Cancer Research Center, Medical College, Xiamen University, 422 Siming South Road, Xiamen 361005, China;

[2]School of Life Science, Xiamen University, 422 Siming South Road, Xiamen 361005, China;

[3]Zhongshan Hospital, Xiamen University, Lakeside South 201-209, Xiamen 361004, China;

[4]These authors contributed equally to this work;

[5]Corresponding author: Dr. Guohong Zhuang, Anti-Cancer Research Center, Medical College, Xiamen University, 422 Siming South Road, Xiamen 361005, China. Tel: +86-592-2180-587; Fax: +86-592-2186-731; E-mail: zhuangguohong@yahoo.com.cn

Received Feb 20, 2009. Accepted Aug 10, 2009.

© 2009 Chinese Society of Immunology and University of Science & Technology of China

Abbreviations: FasL, Fas ligand; RGD, arginine-glycine-aspartic acid; HCC, hepatocellular carcinoma; H22, hepatocellular carcinoma 22; H9101, human hepatocellular carcinoma 9101; ADM, adriamycin; mAb, monoclonal antibody; TUNEL, terminal deoxynucleotidyl transferase-mediated dUTP-biotin nick end-labeling; TNF, tumor necrosis factor.

non-lymphoid cells (5), suggesting that Fas-FasL system may play an important role in the privileged status (6). These findings may indicate that gene transfer of FasL induces apoptotic responses.

Despite the impressive results obtained with various animal models, the clinical use of FasL as an anticancer drug is limited by potential systemic toxicity. For this reason, FasL can be administered to patients only regionally. Regional administration of relatively high doses of TNF in combination with chemotherapeutic drugs has produced high-response rates in patients with advanced limb tumors (7-9), as well as regression of primary and metastatic tumors confined to the liver (10). These results are of particular interest, because they show that, in principle, the antitumor effects of FasL may be exploited therapeutically in humans with greater success if sufficient dose levels can be attained locally, and if the organism can be exempted from the systemic toxic effects.

The tripeptide sequence Arg-Gly-Asp (RGD) is a well known motif that recognizes and interacts with integrins, a family of transmembrane heterodimeric glycoproteins composed of one α and one β subunit (11). Proteins that contain the RGD attachment site, together with the integrins that serve as receptors for them, constitute a major recognition system for cell adhesion (12). The RGD sequence is the cell attachment site of a large number of adhesive proteins in the extracellular matrix, blood, and cell surface, and nearly half of the more than 20 known integrins recognize and bind to related sequences in their adhesion protein ligands (13). The integrin-binding activity of adhesion proteins can be reproduced by short synthetic peptides containing the RGD sequence. Such peptides promote cell adhesion when insolubilized onto a surface and inhibit it when presented to cells in solution. As the integrin-mediated cell attachment influences and regulates cell migration, growth, differentiation, and apoptosis, RGD peptides and mimics can be used to probe integrin functions in various biological systems (14).

Kuroda K., Miyata K. and others have reported that the rhTNF mutant V29 has potent antitumor activity with reduced toxicity in mice (15), whereas another mutant, RGD-T, showed decreased gastrointestinal toxicity (16). RGD-T also overcames the detrimental metastasis-enhancing activity of TNF (17). To eliminate systemic toxicity, including the hypotension associated with human TNF-α, we constructed mutant proteins (muteins) by means of genetic engineering. A novel mutein, F4614, which resulted in the introduction of cell-adhesive Arg-Gly-Asp and 29Arg-->Val, had remarkably reduced hypotensive effects and lower lethality (18).

We have prepared a fusion protein RGD-FasL by recombinant DNA technology and investigated its *in vitro* and *in vivo* antitumor activity. Since RGD-based anti-angiogenic therapies are currently under development, and cyclic Arg-Gly-Asp peptide can also serve as a ligand in human nuclear medicine, optimization of its specificity and drug delivery options is of major importance for clinical applications.

Materials and Methods

Cell culture and mouse tumor model

Hepatoma H22 cells were obtained from the China Center for Type Culture Collection, (CCTCC, Wu Han, China); H9101 cells (Human hepatocellular carcinoma cells) were maintained in our laboratory. H22 and H9101 cells were cultured in RPMI 1640, 1% L-glutamine, 1% penicillin-streptomycin, and 10% fetal calf serum (Wako Pure Chemical Ind., ltd., Japan). The cells were maintained at 37°C in an atmosphere of 5% CO_2 in humidified air. Inbred BALB/c wild-type (WT) mice were purchased from Animal Center for SIAS (Shanghai, China). They were bred and maintained at the Animal Research Central of Xiamen University. All experiments were performed in accordance with guidelines set out by the animal experimental ethics committee.

Expression and purification of recombinant FasL and RGD-FasL

First, the FasL fragment was released from the FasL-pET22b(+) plasmid by polymerase chain reaction (PCR) amplification using the upstream primer F1 (5'-CAG CAG CCC TTC AAT TAC CC-3') and the downstream primer F18 (5'-GCT GCT CGA GCT TAT ATA AGC-3'). Overlapping PCR was performed to link RGD with FasL. Finally, the full-length RGD-FasL gene was obtained by PCR using primers F2 (5'-GTA GGA TCC TCA TGG GCT GCG ATT GTC G-3') and F18 (5'-GCT GCT CGA GCT TAT ATA AGC-3'). The PCR products and the plasmid were digested with *Bam*HI and *Xho*I restriction enzymes, respectively. This RGD-FasL cDNA was purified by agarose gel electrophoresis and subcloned into the responding sites of the eukaryotic expression plasmid pGEX-5X-1 with T4 DNA ligase. After amplification, the recombinant plasmid DNA was transformed into competent *Escherichia coli* (*E. coli*) BL21 (DE3) and screened for ampicillin sensitivity. Subsequently, the plasmid DNA was extracted. After identification of the plasmid restriction fragments, the positive recombinant clones were sequenced at Shanghai Handsome Biotechnology Ltd. A single positive *E. coli* Bl21 (DE3) pGEX-5X-1/ RGD-FasL clone was incubated in shaker flasks at 37°C in 3 mL Luria Bertani (LB) medium for 18-24 h. For large-scale preparations, a 3 ml aliquot of the overnight culture was added to 250 mL of fresh LB medium and incubated in shaker flasks shaken at 250 rpm at 37°C. When the cell density reached an A600 = 0.6~0.8, recombinant protein expression was induced with isopropylthiogalactoside (IPTG). This induction was optimized under a variety of conditions, such as IPTG concentration, induction time and temperature.

The fusion protein was purified by glutathione-S-transferase-affinity column chromatography (according to the manufacturer's protocols provided by GenScript Corporation) and was identified by sodium dodecyl sulfate-polyacrylamide gel electrophoresis (SDS-PAGE) electrophoresis.

Western blot analysis

FasL protein was resolved on a 15% SDS-PAGE gel under

reducing conditions and was transferred to PVDF membranes. After blocking with 5% non-fat milk for 1 h, the PVDF membrane was incubated with anti-human FasL monoclonal antibody (reserved by our lab). Then, the membrane was washed three times with phosphate buffered saline Tween-20 (PBST), followed by incubation for 1 h with HRP conjugated anti-goat antibody. The membrane was washed and then developed with an enhanced chemiluminescence (ECL) detection system (Cell Signaling, USA), followed by exposure to X-ray film.

Cell adhesion assay

Polyvinyl chloride microtiter plates were coated with RGD-FasL or FasL solutions at various concentrations (60,000, 30,000, 15,000, 7,500, 3,750 and 1,875 ng/ml) (100 μl/well in 150 mM sodium chloride, 50 mM sodium phosphate, pH 7.3) at 4°C overnight, then each well was washed with 0.9% sodium chloride, filled with DMEM containing 2% BSA at 37°C for 45 min, and washed again. Cells were harvested and washed three times with 0.9% sodium chloride, resuspended in incomplete DMEM, and added to FasL or RGD-FasL-coated plates (3×10^4 cells/100 μl well). Then the cells were incubated for 1-1.5 h at 37°C, 5% CO_2. Unbound cells were removed by washing with incomplete DMEM. Adherent cells were fixed with 3% paraformaldehyde, 2% sucrose in PBS (pH 7.3), stained with 0.5% crystal violet, and then quantified by reading the absorbance of each well at 540 nm using a microplate reader.

Analysis of Fas and CD61 expression in tumor cell lines by flow cytometry

H22 cells and H9101 cells (1×10^6 cells/ml) were washed twice with PBS containing 1% (w/v) bovine serum albumin (BSA). They were incubated on ice for 40 min with anti-human Fas (Sigma, USA) and anti-CD61 mAb (Sigma, USA). The cells were washed in cold PBS three times, followed by incubation with (FITC)-conjugated affinity-purified goat anti-rabbit IgG (Sigma, USA) for 30 min on ice. The cells were washed and were then analyzed by a FACSCalibur flow cytometer (Becton Dickinson, USA).

In vitro cytolytic assay

The effects of FasL and RGD-FasL on cell proliferation were measured using an MTT-based assay (Microtiter-tetrazolium, Sigma, USA). Briefly, the cells (5,000/ml) were incubated in triplicate in a 96-well plate (Costar, Cambridge, MA, USA) in the presence of various concentrations of FasL and RGD-FasL (1.5625, 3.125, 6.25, 12.5, 25, 50, and 100 μg/ml) in a final volume of 200 μl for the indicated times. Thereafter, 20 μl of MTT solution (5 g/L) was added to each well and then incubated for 12 h. After centrifugation, the supernatant was removed from each well. The colored formazan crystal produced from MTT was dissolved in 150 ml DMSO. Then, the optical density (OD) value was measured at 490 nm by a multiscanner autoreader (Dynatech MR 5000, Chantilly, VA). The following formula was used: cell proliferation inhibited (%) = [1 - (OD of the experimental samples / OD of the control)] × 100%.

Detection of apoptosis by flow cytometric analysis

To determine cell of apoptosis, FasL/RGD-FasL treated or untreated cells (50 μg/ml, 6 h) were washed in PBS and resuspended in binding buffer at a concentration of 1×10^6 cells/ml. After incubation, 195 μl of the solution was transferred into a 5 ml culture tube with 5 μl annexin V-FITC (BD, USA). The tube was then incubated for 30 min at room temperature in the dark. The cells were washed with binding buffer and resuspended in 190 μl binding buffer, with 10 μl PI added. Finally, the tube was gently vortexed and incubated for another 30 min in the dark. Cells were analyzed by FACSCalibur with CellQuest software.

In vivo animal tumor model experiment

All experiments were performed in accordance with guidelines set out by the Animal Experimental Ethics Committee. Single-cell suspensions (1.0×10^5 cells in 100 μl) of H22 were injected s.c. into the right anterior flank of male BALB/c mice (9-12 weeks old). Tumor volume (V) was measured using the formula ($L \times W^2 \times 0.52$), where L and W are the length and width, respectively. Measurements were made with a vernier caliper. Tumor growth was allowed to a volume of 40-50 mm^3. At this point, mice were randomly assigned to different experimental groups. Group 1 (n = 6) received 0.9% NaCl (200 μl), group 2 (n = 6) received FasL (30 μg/mouse in 200 μl of 0.9% NaCl), group 3 (n = 6) received RGD-FasL (30 μg/mouse in 200 μl of 0.9% NaCl), and group 4 (n = 6) received ADM (30 μg/mouse in 200 μl of 0.9% NaCl) *via i.v.* tail vein injection. Injections were administered once daily. According to our project license, animals had to be sacrificed when tumors became too large, if mice lost >20% of body weight, or at signs of pain.

Blood samples were immediately taken retro-orbitally from all groups to observe the levels of serum alanine transaminase (ALT) and aspartate aminotransferase (AST). Standard procedures were used to determine blood parameters using an automated analyzer according to manufacturer's instructions (Cobas Integra 400, Roche Analytics, Germany).

Tumors and livers were excised and fixed in 4% buffered paraformaldehyde solution before embedding in paraffin. Tumor sizes are shown as mean ± SE (6 animals/group). Antitumor activity was assessed by the inhibition rate (IR) of tumor growth 18 days after implantation. The tumor growth inhibition rate (IR) was calculated as follows: IR = (1-T/C) × 100%. Where T is the mean tumor volume in the group treated with FasL or RGD-FasL, and C is the mean tumor volume in the control group treated with saline.

Hematoxylin-and-eosin staining (H&E) analysis

To distinguish antitumor effect of FasL *in vivo*, H&E staining was used. Tumor and liver tissues were harvested after the mice died (n = 6/group). The H&E stained tissues were examined for evidence of necrotic cells, tumor cells, or apoptotic cells. H&E-stained sections were viewed using an

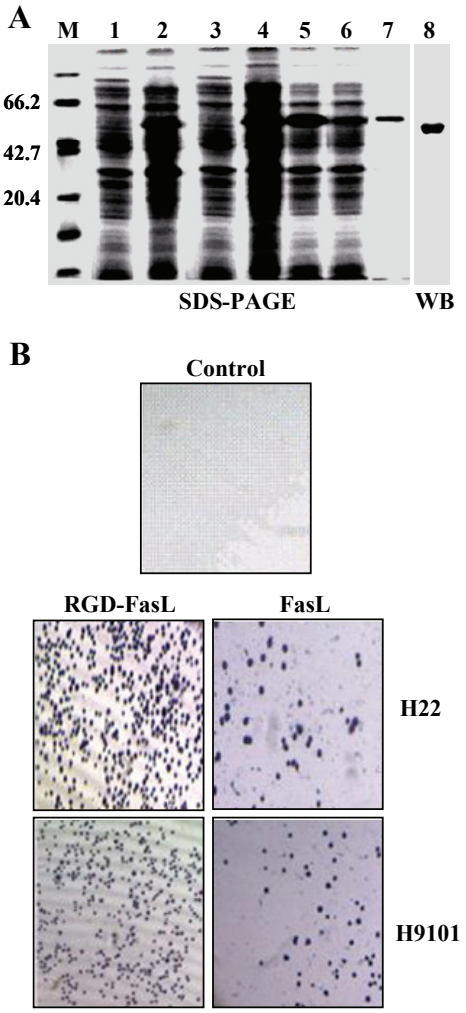

Figuer 1. Recombinant RGD-FasL protein purification and activity identification. (A) Purified RGD-FasL proteins were analyzed by SDS-PAGE or Western blot. Lane M, molecular weight markers; Lane 1, empty vector induced without IPTG; Lane 2, empty vector induced with isopropylthiogalactoside (IPTG); Lane 3, recombinant plasmid induced without IPTG; Lane 4, recombinant plasmid induced with 0.5 mM IPTG; Lane 5, supernatant protein of the recombinant plasmid subjected to IPTG induction and ultrasonic treatment; Lane 6, insoluble protein of the recombinant plasmid subjected to IPTG induction and ultrasonic treatment; Lane 7, recombinant protein purified by glutathione-S-transferase chromatography column; Lane 8, Western blot analysis of recombiant RGD-FasL protein. (B) Cell adhesion assay was performed as described in Materials and Methods. Microtiter wells were coated with 30 mg/ml RGD-FasL or FasL and seeded with H22 and H9101 cells. After 1.5 h, cell adhesion was measured.

Olympus BHT microscope (Melville, NY, USA).

In situ terminal deoxynucleotidyl transferase assay (TUNEL)
Cell apoptosis, were examined by TUNEL method using the Apop Tag *in situ* apoptosis detection Kit (Chemicon International, Inc., Temecula, CA). This method can detect fragmented DNA ends of apoptotic cells. Briefly, the paraffin embedded sections were deparaffinized in xylene and rehydrated in a graded series of ethanol baths. The sections were treated with 20 mg/ml of proteinase K in distilled water for 10 min at room temperature. The tumor tissues were fixed in 1% paraformaldehyde for 10 min. To block endogenous peroxidase, the slides were incubated in methanol containing 0.3% hydrogen peroxide for 20 min. The remaining procedures were performed according to the instructions provided by the manufacturer. To quantify the degree of apoptosis, apoptotic cells were counted by three independent observers who were blinded to the experimental protocol. The apoptotic index was expressed as the percent of the total number of myocardial cells.

Statistical analysis
Data were presented as the mean ± SD per group. Statistical analysis was made for multiple comparisons using analysis of variance and Student's *t*-test. A p-value < 0.05 was considered to be statistically significant.

Results

Production of recombinant FasL and RGD-FasL
The *E. coli* expression system was used to prepare the inclusion form of the RGD-FasL fusion protein. After isolation and purification, the purity of the target protein was more than 95%. The mobility of the purified protein, as determined by SDS-PAGE, was observed at a molecular weight of 62 kDa (Figure 1A). As shown in Figure 1A, the RGD-FasL migrated at the expected molecular weight of 62 kDa, and no degradation was observed. Western blot analysis confirm the production of recombinant RGD-FasL protein using a goat anti-human FasL antibody.

RGD-FasL promotes cell adhesion and spreading
To assess whether the RGD domain of RGD-FasL is functional and accessible to integrins, we compared their cell pro-adhesive properties with a cell adhesion assay. This assay takes advantage of the fact that RGD is the minimal recognition sequence of many integrins and serves as an adhesion motif for them. To this aim, microtiter wells were coated with various amounts of RGD-FasL or FasL and seeded with H22 and H9101 cells. After 1.5 h, cell adhesion was measured. We observed that adhesion and spread of the H22 and H9101 cells on RGD-FasL-coated plates was much greater than that on FasL-coated plates (Figure 1B). These results strongly suggest that the RGD domain of RGD-FasL was sufficiently folded and able to interact with adhesion receptors, most likely integrins, on the cell membrane.

Surface expression of Fas and CD61 in different cell lines
The tripeptide sequence Arg-Gly-Asp (RGD) is a well known motif recognizing and interacting with integrins, a family of transmembrane heterodimeric glycoproteins composed of one α and one β subunit; the β subunits are also called CD61. We examined the cell-surface expression of Fas and CD61 in different cell lines by flow cytometry. As represented in

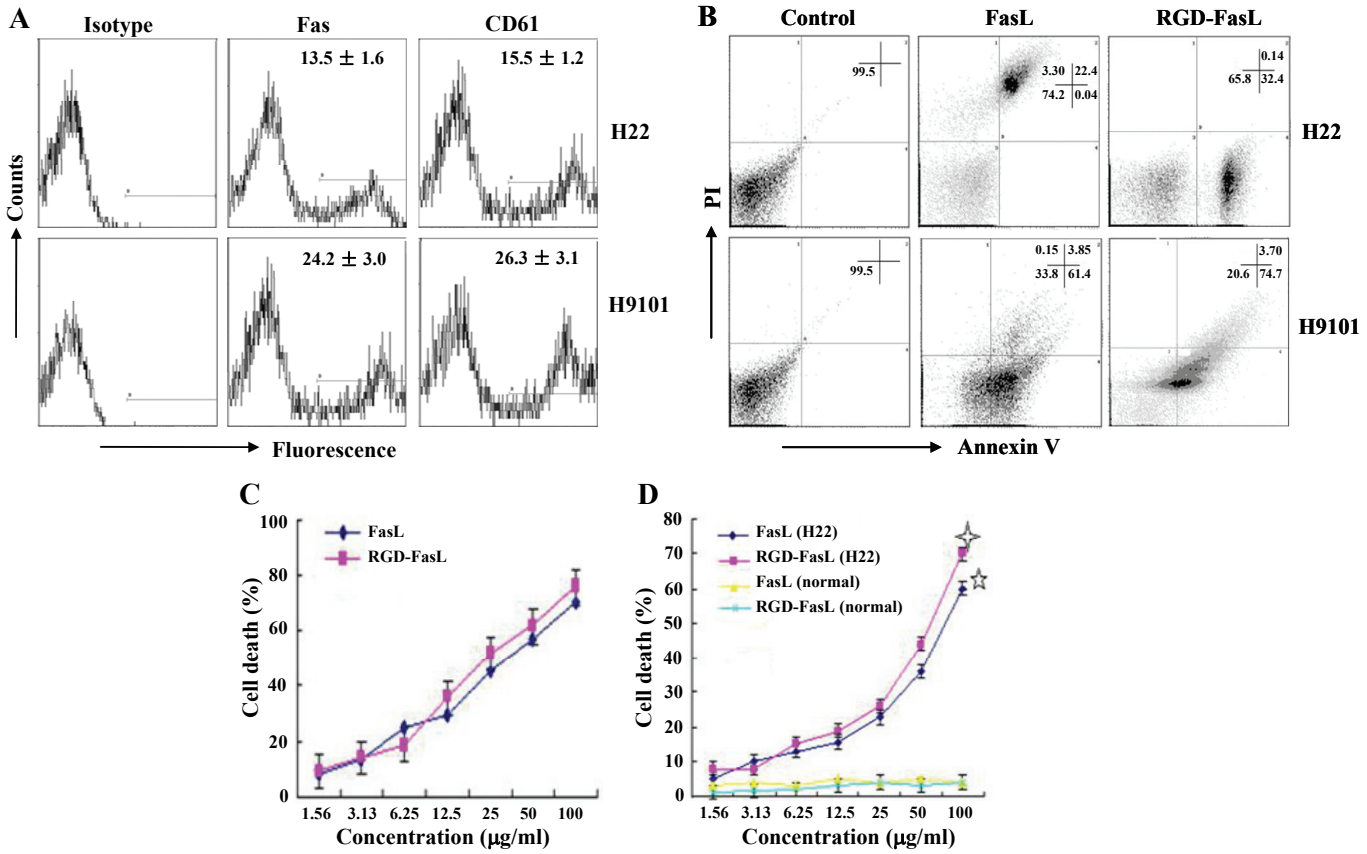

Figure 2. Analysis of *in vitro* activity of RGD-FasL and FasL. (A) Cell surface expression of Fas and H9101 on cell lines H22 and H9101 measured by flow cytometry. (B) Treatment with FasL or RGD-FasL induces apoptosis in H22 and H9101 cells. Treatment of FasL (50 μg/ml) or RGD-FasL (50 μg/ml) for 24 h induced apoptosis in H22 and H9101 cells, as revealed by annexin V-FITC staining assay. (C, D) The inhibition rate of H9101 cells (C) and H22 cells and mouse normal hepatic cells (D) treated with RGD-FasL and FasL. The cells line were incubated for 12 h with 1.5625, 3.125, 6.25, 12.5, 25, 50, 100 μg/ml RGD-FasL or FasL. Cell growth was determined by the MTT assay. Data are expressed as mean ± SD.

Figure 2, approximately 24.2% of H22 cells and 13.5% of H9101 cells expressed Fas, and 26.3% of H22 cells and 15.5% of H9101 cells expressed CD61 (Figure 2A).

Cytotoxic effects of FasL/RGD-FasL on tumor cell lines

To quantify apoptosis, we utilized the annexin V-fluorescein isothiocyanate (FITC) staining assay, which reports the loss of the phosphatidylserine asymmetry of the plasma membrane at an early stage of apoptosis. Both H22 and H9101 cell lines underwent synergistic apoptosis upon 24-h treatment with RGD-FasL or FasL. As shown in Figure 2B a significant increase in apoptosis was induced in cells treated with RGD-FasL or FasL compared to those that were untreated.

To test whether our products were functionally active and capable of inducing cell death and apoptosis, we measured their activity on H22 and H9101 cells. The cytotoxic effects of FasL and RGD-FasL on both of the tumor cell lines were dose-dependent. The 50% inhibition concentration (IC50) values of H9101 cells at 12 h were 26.53 μg/ml (RGD-FasL) and 33.67 μg/ml (FasL) (Figure 2C). The IC50 values of H22 cells at 12 h were 59.63 μg/ml (RGD-FasL) and 92.34 μg/mL (FasL). H9101 cells showed the same sensitivity to RGD-FasL as to FasL ($p > 0.05$), whereas H22 was more sensitive to RGD-FasL than to FasL ($p < 0.05$) (Figure 2D). Both RGD-FasL and FasL have no effect on normal mouse liver cells. However, the sensitivities of the H22/H9101 tumor cell lines to FasL/RGD-FasL differed among experimental groups.

Antitumor effects of FasL and RGD-FasL on mice with H22 tumor

In order to determine whether RGD-FasL had a more potent antitumor activity and reduced toxicity compared with FasL, we evaluated the antitumor effects of the FasL molecules determined in BALB/c mice bearing 40-50 mm^3 H22 tumors (Figure 3). The groups were injected daily (*i.v.*) with 30 μg of recombinant human FasL or RGD-FasL. Both RGD-FasL and FasL clearly demonstrated antitumor activity in this experiment. Tumor growth was monitored daily by measuring the tumor volumes with calipers, as described previously. The tumor inhibition rates (IR) of RGD-FasL and

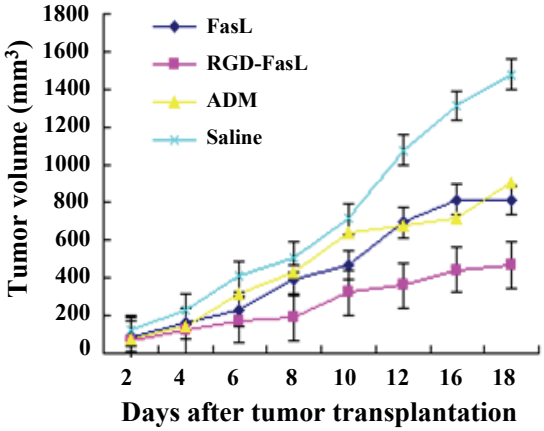

Figure 3. The effects of FasL and RGD-FasL on mice with H22 tumors. Single-cell suspensions (1.0×10^5 cells in 100 μl) of H22 were injected *s.c.* into the right anterior flank of male BALB/c mice (9-12 weeks old). Tumor growth was allowed to a volume of 40-50 mm^3. At the different time point, mice were randomly assigned to different experimental groups. Group 1, FasL (30 μg/mouse in 200 μl of 0.9% NaCl); Group 2, RGD-FasL (30 μg/mouse in 200 μl of 0.9% NaCl); Group 3, ADM (30 μg/mouse in 200 μl of 0.9% NaCl) *via i.v.* tail vein injection; Group 4, 0.9% NaCl (200 μl). Injections were treated once daily. Data are the means ± SE for six mice in each group.

FasL calculated from the tumor weight on day 18 post-tumor transplantation were 68.4% ($p < 0.001$ *vs.* vehicle; *t*-test) and 45.2% ($p < 0.001$ *vs.* vehicle; *t*-test), respectively. Treatment using RGD-FasL displayed an obvious suppressive effect on the HCC tumor model as compared to treatment with FasL ($p < 0.05$). In addition, in this tumor model, treatment of RGD-FasL mice did not lead to an acute liver toxicity as analyzed by ALT and AST activities in the serum. Mice treated with FasL had a moderate increase in AST and ALT serum activities compared to the control group ($p < 0.01$) (Table 1). In the RGD-FasL treated group, no significant treatment-related toxicity in living mice was observed during or after cessation of treatment. In particular, no clinical signs indicating major embolism or stroke (dyspnea, asymmetrical movements, and sudden death) occurred.

Analysis of toxicity of RGD-FasL and FasL

We previously showed that RGD-FasL and FasL induced significant cytotoxicity in H22 and H9101 cells after 24 h treatment. In general, cells undergoing apoptosis display a characteristic pattern of structural changes in the nucleus and the cytoplasm, including rapid blebbing of the plasma membrane and nuclear disintegration. Such cases of nuclear disintegration are associated with extensive chromatin damage and DNA-cleavage into oligonucleosomal length DNA fragments. Detection and quantification of myocardial apoptosis in all experimental cell lines was performed by TUNEL. H&E stain was used to microscopically observe and distinguish died cells from normal cells. The nucleus was stained purple blue, and the cytoplasm and the extracellular

Table 1. Serum ALT/AST analysis of RGD-FasL, FasL and saline treated H22-bearing mice.

	Saline	FasL	RGD-FasL
ALT (IU/L)	48 ± 7	69 ± 8	50 ± 6
AST (IU/L)	81 ± 6	145 ± 9	90 ± 5

Blood samples were collected retro-orbitally from all the treated groups to detect the levels of serum alanine transaminase (ALT) and aspartate aminotransferase (AST). Standard procedures were used to determine blood parameters using an automated analyzer according to the manufacturer's instructions. Data are represented as means ± SD.

matrix were stained red. Necrotic tissues were stained red without structural material, and the karyotin vanished. In this study, compared with the control group, at high magnification, irregular multifocal necrosis were seen in RGD-FasL/FasL/ADM treated group respectively, irregular coagulation necrosis, cellular outline can be seen in nidus in control group, irregular multiforal necrosis were seen in RGD-FasL/FasL/ ADM treated group. (Figure 4I)

In order to tell tumor cellular apotosis from died cell , TUNEL were used, TUNEL-positive apoptotic cells rarely occurred in control animals. Apoptosis was observed to be induced in the cell lines in response to FasL and RGD-FasL by FCM, In tumor tissue, cells undergoing apoptosis were subsequently examined using a fluorescent microscope after TUNEL staining. RGD-FasL and FasL-treated tumor cells showed nuclear chromatin condensation and fragmentation with positive TUNEL signal, red staining indicates DNA stained by PI. Green indicates dUTP end-labeled by FITC. Cells in which the red and green staining overlap are apoptotic, Tumor tissues treated by RGD-FasL/FasL had more apoptotic cells and this results are in accordance with H&E stain (Figure 4II).

Whereas the hepatic tissue section stained with H&E demonstrated few apoptotic and necrotic cells in the RGD-FasL group compared to the ADM and FasL groups. In brief, RGD-FasL has a lower cytotoxic effect than FasL based on the number of normal hepatic cells, and the extent of necrosis was obviously decreased (Figure 4III).

Discussion

FasL is known to directly induce cytotoxicity against tumor cells. However, limitations for the use of FasL fused to antibodies include its nonspecific uptake by the reticuloendothelial system, such as the liver and spleen, resulting in toxicity of these organs. The identification of molecular markers that differentiate newly formed capillaries from their mature counterparts has paved the way for targeted delivery of cytotoxic agents to the tumor vasculature (19). The RGD sequence of some adhesion molecules is recognized by several cell surface integrins (20). In our study, the RGD peptide used for the construction of the RGD-FasL fusion protein has a conformationally restrained RGD sequence that binds to αVβ3 with specificity and high

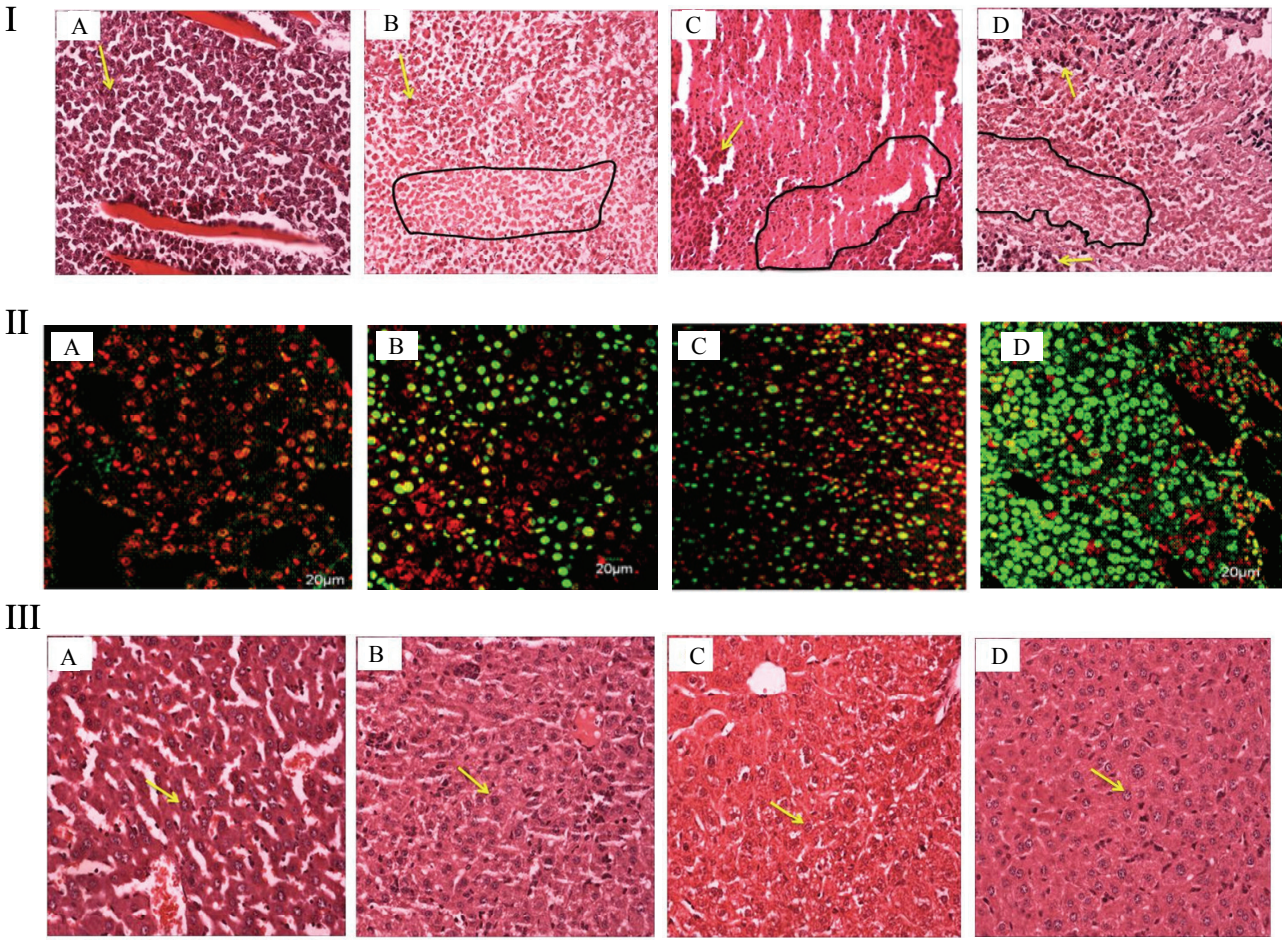

Figure 4. Toxicity analysis of RGD-FasL and FasL.

I, H&E staining of tumor tissues of H22-bearing mice. The tumor tissues were harvested after the mice died (n = 6/group) and were examined histologically for evidence of neointimal hyperplasia and vascular remodeling using routine H&E. (A) mice treated with physiological saline (0.9% NaCl 200 μL); B: treated with FasL (30 μg/mouse in 200 μl of 0.9% NaCl); C: treated with RGD-FasL (30 μg/mouse in 200 μL of 0.9% NaCl); D: treated with ADM (30 μg/mouse in 200 μL of 0.9% NaCl); Magnification × 40. Circle indicates death district of tumor cells, arrow indicates tumor cells.

II, Analysised apoptosis of tumor bearing mice byTUNEL staining

RGD-FasL and FasL-treated tumor cells showed nuclear chromatin condensation and fragmentation with positive TUNEL signal, red staining indicates DNA stained by PI. Green indicates dUTP end-labeled by FITC. Cells in which the red and green staining overlap are apoptotic. (A) control group (0.9% NaCl 200 μl); (B) FasL treated group (30 μg/mouse in 200 μl of 0.9% NaCl); (C) RGD-FasL treated group (30 μg/mouse in 200 μL of 0.9% NaCl); (D): ADM treated group (30 μg/mouse in 200 μl of 0.9% NaCl). Magnification × 400.

III, H&E staining of liver tissues of differently treated H22-bearing mice.

(A) Liver section of physiological saline treated H22-bearing mice (0.9% NaCl 200 μl); (B) Liver section of FasL treated H22-bearing mice (30 μg/mouse in 200 μl of 0.9% NaCl); (C) Liver section of RGD-FasL treated H22-bearing mice (30 μg/mouse in 200 μl of 0.9% NaCl); (D) section Liver of ADM-treated H22-bearing mice (30 μg/mouse in 200 μl of 0.9% NaCl). Magnification × 400.

affinity (21). RGD-FasL carries an αVβ3-selective ligand, allowing active targeting and delivery of effector substances to sites of tumor angiogenesis. RGD-FasL has a greater cytotoxic effect on the H22 and H9101 cell lines than FasL. It has been shown recently that the RGD peptide binds αVβ3 integrin expressed by both tumor cells and tumor endothelial cells (22). H22 cells used in our *in vivo* experimental model express β3 integrins, which was confirmed by flow cytometric analysis. Considering that apoptosis plays a central role in the regulation of hepatocellular carcinoma tissue homeostasis, the imbalance between cell death and proliferation in favor of cell survival could result in tumor formation. One of the commonly employed strategies in experimental gene therapy for cancer is to specifically target death receptors on tumor cells to trigger apoptosis (23). We examined the antiproliferative activity of RGD-FasL against two tumor cell lines. Evidently, their antiproliferative effects were dose-dependent. These results suggested that the

antiproliferative activity of RGD-FasL may be due to direct toxicity to tumor cell. Interestingly, we observed that the sensitivities of H22 and H9101 cell lines to FasL/RGD-FasL were statistically different in the different experimental groups. We suspected that the structure and differential binding activities of RGD to its receptors (integrins) on tumor cells could change the activity of FasL, thereby influencing the cytotoxic effects of the RGD-FasL complex. The results, however, demonstrated that, similar to FasL, RGD-FasL was functional and was able to induce apoptosis in the two tumor cell lines. The data summarized under optimal experimental conditions assessed by flow cytometry are consistent with the results obtained with the MTT assay. The results of the *in vitro* experiments suggest that the RGD moiety of RGD-FasL improves the amount and the persistence of this cytokine in targeted cells. On the other hand, the strong cytolytic activity of RGD-FasL on H22 cells implies that RGD-FasL can also bind FasL receptors and trigger death signals. The finding that the *in vitro* biological activity of RGD-FasL is decreased by co-incubation with an excess amount of free RGD peptide suggests that the improved activity of RGD-FasL is related to targeting. These findings suggest that the improved properties of RGD-FasL depend on the targeted delivery of FasL to RGD or FasL receptors and not to unspecific mechanisms related to NH2-terminal extension.

In vivo treatment of mice bearing H22 resulted in significant tumor growth retardation. In the present study, the antitumor effects of FasL were exploited therapeutically with great success sufficient dose levels can be attained locally, and the organism can be shielded from systemic toxic effects. Nevertheless, re-growth of tumors was observed after cessation of treatment. This phenomenon might be overcome by a better formulation or scheduling of the fusion protein or combination with other therapeutic modalities. As with most approaches targeting the tumor vasculature with coaguligands, the one presented here could not completely inhibit tumor re-growth. To address this problem, we would propose a combination therapy either with cytotoxic agents (e.g., doxorubicin) or local radiation. Besides these modifications, the use of RGD peptides might further enhance potency because of the known higher affinity of cyclic RGD peptides for integrins (24). The specificity of our approach for targeting integrins on tumor endothelium is underlined by the lack of apparent side effects. RGD-FasL appears to have more selective activity towards tumor cells compared with FasL. Thus, RGD-FasL might be expected to have better antitumor properties than FasL in tumor patients. In conclusion, our results demonstrate that RGD-FasL has *in vivo* and *in vitro* anti-tumor properties and has a more effective activity on hepatocellular carcinoma than FasL. RGD-FasL has a lower cytotoxic effect on normal hepatic cells, and the extent of necrosis was obviously decreased.

Acknowledgement

This work was supported by a grant from the Natural Science Foundation of Fujian Province (No.C0710046).

References

1. Farazi PA, DePinho RA. Hepatocellular carcinoma pathogenesis: from genes to environment. Nat Rev Cancer. 2006;6:674-687.
2. Shen DW, Lu YG, Chin KV, Pastan I, Gottesman MM. Human hepatocellular carcinoma cell lines exhibit multidrug resistance unrelated to MRD1 gene expression. Cell Sci. 1991;98:317-322.
3. Doci R, Bignami P, Bozzetti F, Bonfanti G, Audisio R, Colombo M. Intrahepatic chemotherapy for unresectable hepatocellular carcinoma. Cancer. 1988;61:1983-1987.
4. Suda T, Takahashi T, Golstein P, Nagata S. Molecular cloning and expression of the Fas ligand, a novel member of the tumor necrosis factor family. Cell. 1993;75:1169-1178.
5. Bellgrau D, Gold D, Selawry H, Moore J, Franzusoff A, Dukeb RC. A role for CD95 ligand in preventing graft rejection. Nature. 1995;377:630-632.
6. Pinkoski MJ, Green DR. Cloak and dagger in the avoidance of immune surveillance. Curr Opin Gene Dev. 2000;10:114-119.
7. Lienard D, Ewalenko P, Delmotte JJ, Renard N, lejeune FJ. High-dose recombinant tumor necrosis factor α in combination with interferon γ and melphalan in isolation perfusion of the limbs for melanoma and sarcoma. J Clin Oncol. 1992;10:52-60.
8. Eggermont AM, Schraffordt Koops H, Lienard D, et al. Isolated limb perfusion with high-dose tumor necrosis factor-α in combination with interferon-γ and melphalan for nonresectable extremity soft tissue sarcomas: a multicenter trial. J Clin Oncol. 1996;14:653-2665.
9. Fraker DL, Alexander HR, Andrich M, Rosenberg SA. Treatment of patients with melanoma of the extremity using hyperthermic isolated limb perfusion with melphalan, tumor necrosis factor, and interferon γ: results of a tumor necrosis factor dose-escalation study. J Clin Oncol. 1996;14:479-489.
10. Alexander HR, Bartlett DL Jr, libutti SK, Fraker DL, Moser T, Rosenberg SA. Isolated hepatic perfusion with tumor necrosis factor and melphalan for unresectable cancers confined to the liver. J Clin Oncol. 16:1479-1489,
11. Qin J, Chen D, Hu H, Qiao M, Zhao X, Chen B. Body distributioin of RGD-mediated liposome in brain-targeting drug delivery. Yakugaku Zasshi. 2007;127:1497-1501.
12. Villard V, Kalvuzhniv O, Riccio O, et al. Synthetic RGD containing α-helical coiled coil peptides promote integrin dependent cell adhesion. J Pept Sci. 2006;12:206-212.
13. Wu Pl, Lee SC, Chuang CC, et al. Non-cytotoxic cobra cardiotoxin A5 binds to αvβ3 integrin and inhibits bone resorption. Identification of cardiotoxins as non-RGD integrin binding proteins of the ly-6 family. J Bio Chem. 2006;281: 7937-7945.
14. Lu X, Lu D, Scully MF, Kakkar VV. Integrins in drug targeting-RGD templates in toxins. Curr Pharm Des. 2006;12: 2749-2769.
15. Kuroda K, Miyata K, Shikama H, et al. Novel muteins of human tumor necrosis factor with potent antitumor activity and less lethal toxicity in mice. Int J Cancer. 1995;63:152-157.
16. Shikama H, Miyata K, Sakae N, et al. A novel mutein of TNFα containing the Arg-Gly-Aspsequence shows reduced toxicity in intestine. Mediators Inammation. 1994;3:111-116.
17. Miyata K, Mitsuishi Y, Shikama H, et al. Overcoming the metastasis-enhancing potential of human tumor necrosis factor α by introducing the cell-adhesive Arg-Gly-Asp sequence.

Interferon Cytokine Res. 1995;15:161-169.
18. Shikama H, Miyata K, Sakae N, et al. Novel mutein of tumor necrosis factor α (F4614) with reduced hypotensive effect. Interferon Cytokine Res. 1995;15:677-684.
19. Weissleder R, Kelly K, Sun EY, Shtatland T, Josephson L. Cell-specific targeting of nanoparticles by multivalent attachment of small molecules. Nat Biotechnol. 2005;23:1418- 1423.
20. Shukla R, Thomas TP, Peters J, Kotlyar A, Myc A, Baker JR. Tumorangiogenic vasculature targeting with PAMAM dendrimer-RGD conjugates. Chem Commun (Camb) 2005; 5739-5741.
21. ArapW, Pasqualini R, Ruoslahti E. Cancer treatment by targeted drug delivery to tumor vasculature in a mousemodel. Science. 1998;279:377-380.
22. Pasqualini R, Koivunen E, Ruoslahti E. αV integrins as receptors for tumor targeting by circulating ligands. Nat Biotechnol. 1997;15:542-546.
23. Adamson GM, Billings RE. Tumor necrosis factor: receptor binding and expression of receptors in cultured mouse hepatocytes. Pharmacol Exp Ther. 1994;269:367-373.
24. Koivunen E, Gay DA, Ruoslahti E. Selection of peptides binding to the a5h1 integrin from phage display library. Biol Chem. 1993;268:20205-20210.